

# Locally Constrained Policy Optimization for Online Reinforcement Learning in Non-Stationary Input-Driven Environments

Pouya Hamadani<sup>1</sup> Arash Nasr-Esfahany<sup>1</sup> Siddhartha Sen<sup>2</sup> Malte Schwarzkopf<sup>3</sup> Mohammad Alizadeh<sup>1</sup>

## Abstract

We study online Reinforcement Learning (RL) in non-stationary input-driven environments, where a time-varying exogenous input process affects the environment dynamics. Online RL is challenging in such environments due to “catastrophic forgetting” (CF). The agent tends to forget prior knowledge as it trains on new experiences. Prior approaches to mitigate this issue assume task labels (which are often not available in practice) or use off-policy methods that can suffer from instability and poor performance.

We present Locally Constrained Policy Optimization (LCPO), an on-policy RL approach that combats CF by anchoring policy outputs on old experiences while optimizing the return on current experiences. To perform this anchoring, LCPO locally constrains policy optimization using samples from experiences that lie outside of the current input distribution. We evaluate LCPO in two gym and computer systems environments with a variety of synthetic and real input traces, and find that it outperforms state-of-the-art on-policy and off-policy RL methods in the online setting, while achieving results on-par with an offline agent pre-trained on the whole input trace.

A major hurdle has been the gap between simulation and reality, where the environment simulators do not match the real-world dynamics. Thus, recent work has turned to applying RL in an online fashion, i.e. continuously train and use an agent in a live environment (Zhang et al., 2021; Gu et al., 2021).

While online RL is difficult in and of itself, it is particularly challenging in *non-stationary* environments, where the characteristics of the environment changes over time. In this paper we consider problems where the source of the non-stationarity is an observed exogenous input process that varies over time and exposes the agent to different environment dynamics. Such input-driven environments (Mao et al., 2018b) appear in a variety of applications. Examples include computer systems subject to incoming workloads (Mao et al., 2018a), locomotion in environments with varying terrains and obstacles (Heess et al., 2017), robots subject to external forces (Pinto et al., 2017), and more.

On the one hand, since the cause of the non-stationarity is observed, an RL agent should in theory be able to learn a *single* policy that works well for different input behaviors. In particular, if we knew about all possible input behaviors beforehand, it would be straightforward to train an effective RL policy offline. However, online RL in such environments is much more difficult. The main problem is Catastrophic Forgetting (CF) (McCloskey & Cohen, 1989), a common pitfall of sequential learning using function approximators like Neural Networks (NNs). NNs tend to “forget” their past knowledge in online sequential learning problems. In particular, on-policy RL algorithms follow a sequential learning procedure that cannot retrain on past data and are hence vulnerable to CF.

A growing body of work focuses on mitigating CF, especially in supervised learning and task-based settings (Rusu et al., 2016; Kirkpatrick et al., 2017; Schwarz et al., 2018; Farajtabar et al., 2019) where it is assumed that we are given explicit task labels identifying different observed distributions throughout the learning process. Task labels make it easier to prevent the cross-contamination effects that training on one task can have on knowledge learned for other tasks. Only a few works target online RL when task labels (or boundaries) are not available. A common approach in this case is to infer task labels by self-supervised (Nagabandi et al.,

## 1. Introduction

— *Those who cannot remember the past are condemned to repeat it. (George Santayana, The Life of Reason, 1905)*

Reinforcement Learning (RL) has seen success in many different domains (Mao et al., 2017; Haarnoja et al., 2018a; Mao et al., 2019; Marcus et al., 2019; Zhu et al., 2020; Haydari & Yilmaz, 2022), but real-world deployments have been rare.

<sup>1</sup>Computer Science and Intelligence Lab, Massachusetts Institute of Technology, Cambridge, Massachusetts, USA <sup>2</sup>Microsoft Research, New York City, New York, USA <sup>3</sup>Computer Science Department, Brown University, Providence, Rhode Island, USA. Correspondence to: Pouya Hamadani <pouyah@mit.edu>.

2019) or change-point detection approaches (Padakandla et al., 2020; Alegre et al., 2021), which past work has shown to be brittle in practice (Hamadani et al., 2022). Another alternative is off-policy learning, which makes it possible to retrain on past data and improves sample complexity. However, off-policy methods come at the cost of higher hyper-parameter sensitivity and unstable training and are often outperformed by on-policy algorithms in practice (Duan et al., 2016; Gu et al., 2016; Haarnoja et al., 2018b).

We propose LCPO (§4), an on-policy RL approach that “anchors” policy output on old experiences (state, input pairs) while optimizing on current experiences. Unlike prior work, LCPO does not rely on task labels and only requires an Out of Distribution (OOD) detector, i.e. a function that recognizes old experiences that came from sufficiently different input distributions than the one currently being experienced. LCPO maintains a buffer of past experiences, similar to off-policy methods (Mnih et al., 2013). But it does not use these experiences to optimize the policy. It uses them in a constrained optimization problem that optimizes for expected return on the *current* experiences without forgetting the past. We present three practical algorithms to solve this constrained policy optimization problem (§5). We evaluate LCPO on two environments with real and synthetic data (§6), and show that LCPO outperforms several state-of-the-art on-policy and off-policy baselines and achieves results on par with an offline-trained policy with access to all input traces beforehand. Ablation studies show that LCPO is reasonably immune to variations in the OOD detector’s thresholds.

## 2. Related Work

**CF in Machine Learning (ML) and Deep RL:** Outside of RL, three general approaches exist for mitigating CF; (1) regularizing the optimization to avoid memory loss during sequential training (Kirkpatrick et al., 2017; Kaplanis et al., 2018; Farajtabar et al., 2019); (2) training separate parameters per task, and expanding/shrinking parameters as necessary (Rusu et al., 2016); (3) utilizing rehearsal mechanisms, i.e. retraining on original data or generative batches (Isele & Cosgun, 2018; Rolnick et al., 2019; Atkinson et al., 2021); or combinations of these techniques (Schwarz et al., 2018). For a full review of these approaches, refer to (Parisi et al., 2019).

The first two groups require task labels, and often require each individual task to finish training. The RL answer to rehearsal is off-policy training. However, off-policy RL is empirically unstable, hyperparameter sensitive due to bootstrapping and function approximation (Sutton & Barto, 2018), and often outperformed by on-policy algorithms (when sample-complexity is not an issue) (Duan et al., 2016; Gu et al., 2016; Haarnoja et al., 2018b).

**Non-stationarity in RL:** A long line of work exists on

non-stationary RL that explore subproblems in the space, and a general solution has not been yet been proposed (Khetarpal et al., 2020). The most notable class of approaches attempt to infer task labels, by learning the transition dynamics of the Markov Decision Process (MDP) so far, and detecting a new environment when a surprising sample is observed with respect to the learnt model (Doya et al., 2002; da Silva et al., 2006; Padakandla et al., 2020; Alegre et al., 2021). These methods are effective when environment transitions are abrupt and have fairly well-defined boundary. Prior work has observed that they are brittle and can perform poorly in realistic environments with noisy and hard-to-distinguish non-stationarities (Hamadani et al., 2022). Another recent work assumes a stationary discrete latent Markovian context and learns a model for the generalized MDP, i.e. assumes the underlying environment is piece-wise stationary (Ren et al., 2022). By contrast to these papers, our work does not rely on estimating task labels and does not assume piece-wise stationarity. For a comprehensive review of non-stationary RL, refer to (Khetarpal et al., 2020).

### Constrained optimization and exploration techniques.

LCPO’s constrained optimization formulation is inspired by Trust Region Policy Optimization (TRPO) methods (Schulman et al., 2015). A recent work uses a similar techniques to LCPO-P (one of three LCPO variants) to “edit” neural networks (Sinitin et al., 2020), e.g., to fix errors in certain classification labels. Unlike us, their problem is supervised learning and assumes access to labeled ground truth data. Online RL requires methods to explore newly-encountered environment dynamics. Exploration is orthogonal to LCPO’s main technique but in our experiments we use the automatic entropy regularizer introduced in (Haarnoja et al., 2018c) and find that it works well. LCPO could be combined with more sophisticated techniques such as curiosity-driven exploration (Pathak et al., 2017).

## 3. Preliminaries

### 3.1. Notation

We consider online policy learning in a Non-Stationary Markov Decision Process (NS-MDP) with observed exogenous inputs. Formally, at time step  $t$  the environment has state  $s_t \in \mathcal{S}$  and input  $z_t \in \mathcal{Z}$ . The agent takes action  $a_t \in \mathcal{A}$  based on the observed state  $s_t$  and input  $z_t$ , and receives feedback in the form of a scalar reward  $r_t(s_t, z_t, a_t) : \mathcal{S} \times \mathcal{Z} \times \mathcal{A} \rightarrow \mathbb{R}$ . The environment’s state, the input, and the agent’s action determine the next state,  $s_{t+1}$ , according to a transition kernel,  $T(s_{t+1}|s_t, z_t, a_t)$ . The input  $z_t$  is an independent stochastic process, unaffected by states  $s_t$  or actions  $a_t$ . Finally,  $d_0$  defines the distribution over initial states ( $s_0$ ). This model is fully defined by the tuple  $\mathcal{M} = (\mathcal{S}, \mathcal{Z}, \mathcal{A}, \{z_t\}_{t=1}^\infty, T, d_0, r)$ . The goal of the agent is to optimize the *return*, i.e. a discounted sum of

rewards  $R_0 = \sum_{t=0}^{\infty} \gamma^t r_t$ . This model is very similar to the input-driven environment described in (Mao et al., 2018b).

### 3.2. Online RL

In traditional RL settings, a policy is trained via either simulation or a separate training phase, and then rolled out for usage in testing. On the other hand, an online learning setting starts with the test phase, and the policy must reach optimality within this test phase. Naturally this means that the policy must explore, yielding temporarily low returns, and then enter an exploitation phase. This complicates the definition of a successful online learner: in this work, we primarily seek long-term performance, i.e. the policy eventually attains high returns; secondarily, we seek low transient return loss during exploration. For simplicity, we assume a short grace period in each online learning experiment that allows for free exploration, and rate performance in the long span after the grace period.

In the following sections, we use informal terminology such as *novel input* or *unexplored input* to refer to portions of the input trace  $z_t$  that have not been observed before in the online setting. We do not provide formal definitions because non-stationary behavior is difficult to quantify, and we do not wish to constrain the input trace’s behavior in any way. The input can exhibit arbitrary behavior: e.g., it can fit a predictable pattern or be i.i.d samples, experience smooth or dramatic shifts, follow a piece-wise stationary model, or any mixture of the above. Either way, in this online setting, we have no prior access to the input, environment or a simulator (except with pre-trained models) and we assume no way of characterizing how the input is going to change.

## 4. Locally-Constrained Policy Optimization

Our goal is to learn a policy  $\pi(\cdot, \cdot)$  in an online setting that takes action  $a_t \sim \pi(s_t, z_t)$ , in an NS-MDP characterized by an exogenous input trace exhibiting non-stationary behavior. Online RL in non-stationary environments, even when there are no unobserved elements, is quite challenging and remains an open problem. There are two main problems to solve:

1. When we experience an explored input trace and learn a policy for it, we must guarantee that we will not forget the policy we learned for older inputs, i.e. avoid CF.
2. Learning an optimal policy requires exploration to gauge the best path to optimal returns. When the environment is stationary, this is done once initially and the agent only exploits its knowledge afterwards. In an NS-MDP, upon each new and unexplored portion of the input trace, we must explore again. Exploration is costly and incurs regret, and we ideally would like to only do it once for each novel input.

As an illustrative example, consider the grid-world problem

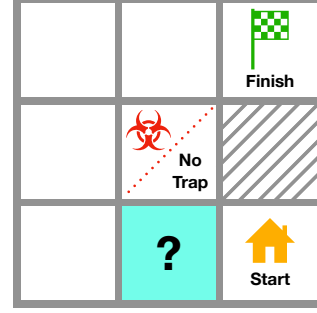


Figure 1. A simple 3x3 grid-world problem with two modes.

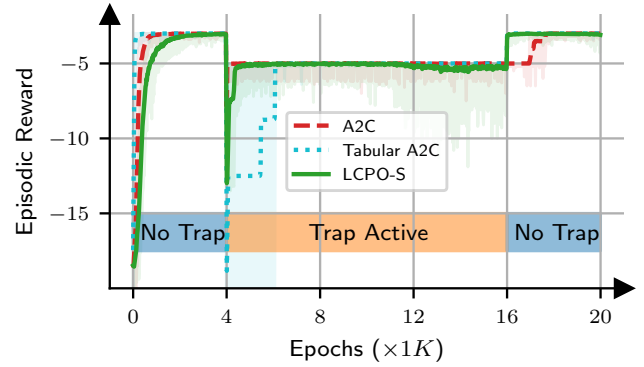


Figure 2. Episodic reward across time in the grid environment.

depicted in Figure 1. In this problem, the agent can move in 4 directions in a 2D grid, while incurring a base negative reward of  $-1$  per step, until it reaches the terminal exit state or fails to within 20 steps. The grid can be in two modes; 1) no trap mode, where the center cell is empty, and 2) trap active mode, where walking into the center cell incurs a reward of  $-10$ . This environment mode is our “input process” in this simple example and the source of non-stationarity. The agent observes its current location and the input, i.e. whether the trap is on the grid or not in every episode (beginning from the start square).

We use the Advantage Actor Critic (A2C) algorithm to train a policy for this environment, while its input changes every so often. When in no trap mode, the closest path passes through the center cell, and the best episodic reward is  $-3$ . In the trap active mode, the center cell’s penalty is too high, and we must go left at the blue cell instead, to incur an optimal episodic reward of  $-5$ . Figure 2 depicts the episodic reward across time and Figure 3 depicts what fraction of the time the policy makes the correct decision to go up in the blue cell when the input is in no trap mode. As observed, the agent initially learns the correct decision for that cell when training in the no-trap mode, but once the input (mode) changes, it begins to forget it. When the mode changes back to the initial no trap mode, the agent behaves sub-optimally for some number of episodes (epochs 16K-18K) before recovering.

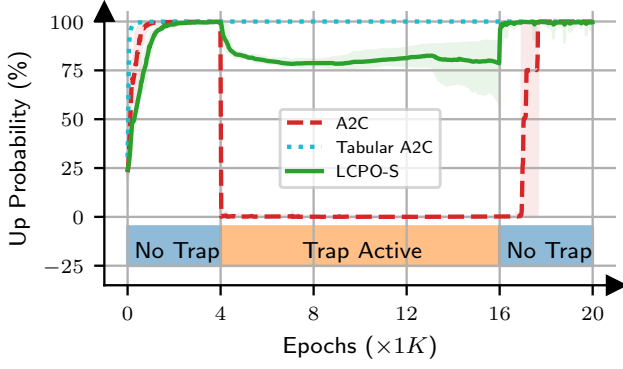


Figure 3. Probability of going up at the blue cell according to the policy, when at ‘No Trap’ mode. Note that in the trap active period, the shown probability is not used in the episode, and is only a measure of how much the agent has forgotten since epoch  $4K$ .

The best approach here would be to train a separate model for each mode (2 models). However, deducing when to train a new model or switch to an old one requires task labels. However, deducing such labels is challenging in practice and methods to infer them, e.g., using change-point detection (Alegre et al., 2021) are brittle in real-world non-stationary problems (Hamadani et al., 2022). We do not assume access to task labels.

This specific problem has a discrete space for states and inputs. Therefore, let us try applying a tabular version of A2C: i.e., the policy and value networks are tables with separate rows for each state  $s_t$  and input mode  $z_t$  (18 total rows). In this case, the policy output, depicted in Figure 3, does not forget its original learning. This is not surprising. When a state-action tuple is used to update the table, it only updates the row pertaining to its own state and input. Therefore, even if the input changes, it will not affect rows belonging to other inputs. Exploration is also not an issue. Any untouched cell by default leads to an exploratory policy and thus any novel input will first trigger exploration. This implies that in order to achieve the same results with neural-network based function approximators, we must ensure that the policy output for other (state, input) pairs (analogous to the cells in the tabular setting) are “anchored” while we update the relevant (state, input) pairs.

Neural networks are parameterized function approximators, and when they are updated with the recursive formulae of policy gradient, they look for the best fit to the current batch of data, potentially changing the entirety of their output space, including outputs on past inputs. Off-policy algorithms, which sample on all past data including past input traces, directly anchor past output with the current batch. Unfortunately, besides the aforementioned weaknesses of off-policy approaches, we shall observe in §6 that they are outperformed by on-policy algorithms in online learning.

Using task labels allows us to anchor the output on past inputs by not changing the parameters relevant to those inputs, but only if the task labels are accurate. In the absence of task labels, we make the case that we only need to know if two inputs  $z_i$  and  $z_j$  are *different*. Assuming we had such a difference detector, we could use it to anchor prior (state, input) pairs in our function approximator when updating newly-experienced ones. We formulate difference detection in the following way: given a batch of recent experiences  $B_r$  and all experiences  $B_a$ , assume a function  $W$  exists such that  $W(B_a, B_r)$  is a distribution for sampling past experiences from  $B_a$  that are dissimilar to the recent batch  $B_r$ . Then, we can anchor policy output on past experiences sampled via  $W(B_a, B_r)$  to not change. We name this approach Locally Constrained Policy Optimization (LCPO). The result for LCPO-S, a variant of LCPO that we discuss in §5, is presented in Figure 3. While it does not retain its policy as perfectly as tabular A2C while in the trap mode, it does sufficiently well to recover near instantaneously upon the second switch.

This raises three questions. First, how is designing a difference detector any easier than inferring task labels? The answer is that in practice, detecting if two input processes are similar or not is often much easier than classifying and clustering them online. In §6 we highlight an example from real-world computer systems, where even a human expert cannot design a hand-crafted task classifier, but detecting similarity or lack thereof is straightforward.

Second, if anchoring aims to mimic tabular policy classes, are we losing the generalization capability that neural networks provide? While we attempt to separate the neural network output for different inputs by anchoring, we are not changing optimization within similar regions of the input process. Thus, neural networks can still generalize across the observed states for similar inputs. Generalizing across widely different inputs requires the a pre-trained offline agent with access to the full input distribution beforehand, such that all input traces are effectively observed together in each training batch (and hence we avoid CF).

Third, how will we perform this anchoring effectively? Approaches with a similar principle exist in prior ML literature in the supervised learning setting, but they use data with ground truth labels for anchoring. In contrast, in RL we do not have ground truth for policy output, and do not know if we have reached convergence on a specific input. In the next section, we discuss three ways to approximately achieve the desired anchoring.

## 5. Methodology

Consider a parameterized policy  $\pi_\theta$  with parameters  $\theta$ . Our task is to choose a direction for changing  $\theta$  such that it improves the policy gradient loss  $\mathcal{L}_{PG}(\theta; B_r)$  on the most



**Algorithm 1** LCPO-S Training

---

```

1: initialize parameter vectors  $\theta_0$ 
2: initialize empty dataset  $B_a$ 
3: for each iteration do
4:   Perform rollouts and store samples to  $B_r$ 
5:   Get anchoring states  $B_{anchor} \leftarrow W(B_a, B_r)$ 
6:    $v_{PG} \leftarrow \nabla_{\theta} \mathcal{L}_{PG}(\theta; B_r)|_{\theta_0}$ 
7:   if  $B_{anchor}$  is not empty then
8:      $g(x) := \nabla_{\theta} (x^T \nabla_{\theta} \mathcal{D}_{KL}(\theta, \theta_{old}; B_{anchor})|_{\theta_0})|_{\theta_0}$ 
9:      $v_{anchored} \leftarrow \text{conjgrad}(v_{PG}, g(\cdot))$ 
10:    if  $\theta_{old} + v_{anchored}$  violates constraints then
11:       $v_{anchored} \leftarrow v_{anchored}/2$ 
12:    end if
13:     $\theta_0 \leftarrow \theta_0 + v_{anchored}$ 
14:  else
15:     $\theta_0 \leftarrow \theta_0 + v_{PG}$ 
16:  end if
17:  add samples to dataset  $B_a \leftarrow B_a + B_r$ 
18: end for
    
```

---

recent batch of experiences  $B_r$ , while the policy is ‘anchored’ on prior samples with sufficiently distinct input distributions,  $W(B_a, B_r)$ . This is formalized as follows:

$$\begin{aligned} \min_{\theta} \quad & \mathcal{L}_{PG}(\theta; B_r) \\ \text{s.t.} \quad & D_{KL}(\theta_0, \theta; W(B_a, B_r)) \leq c_{anchor} \end{aligned} \quad (1)$$

We use KL-divergence as a measure of policy change, and for simplicity of notation we use  $D_{KL}(\theta_0, \theta; W(B_a, B_r))$  as a shorthand for  $\mathbb{E}_{s, z \sim W(B_a, B_r)} [D_{KL}(\pi_{\theta_0}(s, z), \pi_{\theta}(s, z))]$ . Here,  $\theta_0$  denotes the current policy parameters, and we are solving the optimization problem over  $\theta$  to determine the new policy parameters. Ideally, we would target  $c_{anchor} = 0$ , such that any output change on past samples is avoided. However, this would make the problem intractable in general, and thus we allow for a small  $c_{anchor} > 0$ .

To realize  $W(B_a, B_r)$ , we treat it as an out-of-distribution detection (OOD) task. A variety of methods can be used for this in practice (§6). For example, we can compute the Mahalanobis distance, i.e. the normalized distance of each experience’s input, with respect to the average input in  $B_r$ , and deem any distance above a certain threshold OOD.

There are two ways to solve this optimization problem. The first approach, inspired by TRPO (Schulman et al., 2015), is to model the optimization goal with a first-order approximation, i.e.  $\mathcal{L}_{PG}(\theta; \cdot) = \mathcal{L}_0 + (\theta - \theta_0)^T \nabla_{\theta} \mathcal{L}_{PG}(\theta; \cdot)|_{\theta_0}$ , and the constraint with a second order approximation  $D_{KL}(\theta, \theta_0; \cdot) = (\theta - \theta_0)^T \nabla_{\theta}^2 D_{KL}(\theta, \theta_0; \cdot)|_{\theta_0} (\theta - \theta_0)$ . As we are using a trust region method, we must also constrain policy change on the recent states as well, as done in TRPO, but with a more generous bound compared to anchored

states. In total, this approach is formalized as follows:

$$\begin{aligned} \min_{\theta} \quad & (\theta - \theta_0)^T v_{PG} \\ \text{s.t.} \quad & (\theta - \theta_0)^T A (\theta - \theta_0) \leq c_{anchor} \\ & (\theta - \theta_0)^T B (\theta - \theta_0) \leq c_{recent} \end{aligned} \quad (2)$$

where  $A_{ij} = \frac{\partial}{\partial \theta_i} \frac{\partial}{\partial \theta_j} D_{KL}(\theta, \theta_0; W(B_a, B_r))$ ,  $B_{ij} = \frac{\partial}{\partial \theta_i} \frac{\partial}{\partial \theta_j} D_{KL}(\theta, \theta_0; B_r)$  and  $v_{PG} = \nabla_{\theta} \mathcal{L}_{PG}(\theta; \cdot)|_{\theta_0}$ . We name this variant of our approach LCPO-D (D as in double constraints). Two second-order constraints complicate the optimization problem, but we outline the solution in Appendix §A.1. Note that we use the conjugate gradient algorithm, similar to TRPO, to avoid directly computing  $A$  or  $B$  and their inverses.

In practice, we find that the constraint on recent batches is not necessary, since the anchoring constraint is strict enough to also constrain policy change. In that case, we can guarantee the second constraint by a simple line search along the search direction of the constrained optimization problem, which can be derived analytically (§A.1). This leads to almost  $3 \times$  less computation required and garners similar, if not better results. We name this second approach LCPO-S (S as in single constraint). The pseudocode for this method is presented at Algorithm 1.

The third way to uphold the anchoring constraint is to directly add it as term in the loss function. Let us define:

$$\begin{aligned} \mathcal{L}_{anchor}(\theta, \theta_0; B_r, B_a) = \\ \mathbb{E}_{s, z \sim W(B_a, B_r)} [CELoss(\pi_{\theta}(s, z), \pi_{\theta_0}(s, z))] \end{aligned} \quad (3)$$

Where we use the Cross Entropy loss to incentivize policy anchoring. Then, we optimize the following total loss:

$$\min_{\theta} \quad \mathcal{L}_{PG}(\theta; \cdot) + \kappa \cdot \mathcal{L}_{anchor}(\theta, \theta_0; B_r, B_a) \quad (4)$$

This approach is even less compute intensive than LCPO-S, but is not possible in vanilla policy gradient. This is because the gradient direction from  $\mathcal{L}_{anchor}$  is zero when  $\theta = \theta_0$  and will not affect the optimization. Therefore, we have to repeat the gradient update several times before this term has an effect. We use a PPO (Schulman et al., 2017) style optimization method for this purpose, which we call LCPO-P (P stands for proximal).

Overall, LCPO-S garners the best results, and proves effective at battling catastrophic forgetting. However, exploring on new input processes is a tangential but critical problem. While we defer a more principled exploration method for future work, we have found that an automatic entropy regularizer, proposed in (Haarnoja et al., 2018c) can

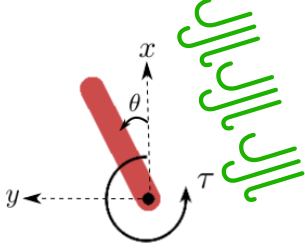


Figure 4. Pendulum-v1 environment with external wind.

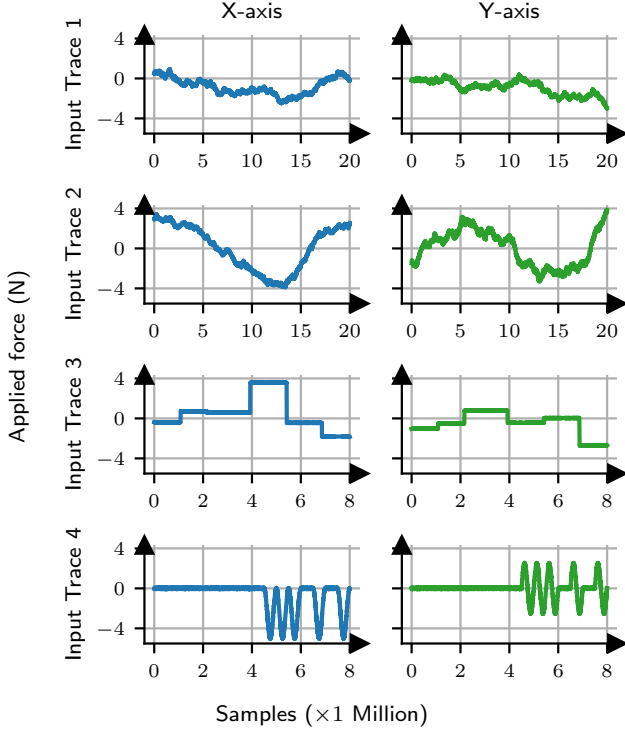


Figure 5. External wind force, per axis and input trace.

maintain enough exploration in the policy to retrain itself upon observing a new input.

## 6. Evaluation

We designed experiments, with both real and synthetic input traces, as an attempt to answer the following questions:

1. How does LCPO compare to on-policy approaches? How close can it get to an optimal policy?
2. How does LCPO compare to state-of-the-art off-policy algorithms?
3. How do the three styles of LCPO compare with one another?
4. How does the accuracy of the OOD sampler  $W(\cdot, \cdot)$  affect LCPO?

To answer the first question, we compare with A2C (Mnih

et al., 2016) and TRPO (single-path) (Schulman et al., 2015), with Generalized Advantage Estimation (GAE) (Schulman et al., 2018) applied. To answer the second question, we compare with Double Deep Q Network (DDQN) (Hasselt et al., 2016) and Soft Actor Critic (SAC) (with automatic entropy regularization, similar to LCPO) (Haarnoja et al., 2018b). We train an “online” and “offline” version for each method, which: 1) online: experiences the non-stationary input, and 2) offline: experiences a stationary environment with that input, by sampling from the entire input in each batch. The offline version acts as the ‘optimal’ policy, i.e. close to the best that LCPO could achieve. In §6.1 we experiment with three versions of LCPO introduced in §5. Finally, for the last question, we assess LCPO-S as we gradually change the OOD sampler, in §6.2. Hyperparameters and neural network structures are noted in Appendices §B.2 and §C.1.

### 6.1. Pendulum locomotion with synthetic inputs

We consider a modified version of Pendulum-v1 from the classic control gym environments (Brockman et al., 2016). The input is an exogenous wind process that creates external force on the pendulum and affects the movement (Figure 4). We append the external wind vectors from the last 3 time-steps to the observation, leading to a 9-dimensional observation space. We create 4 synthetic input traces with the Ornstein–Uhlenbeck process (Uhlenbeck & Ornstein, 1930), piece-wise Gaussian models, or hand-crafted signals with additive noise. These inputs cover smooth, sudden, stochastic, and predictable transitions at short horizons. All inputs are visualized in Figure 5.

To sample past inputs  $W(B_a, B_r)$ , we use L2 distance. If  $\bar{w}_r$  is the average wind vector observed in the recent batch  $B_r$ , we sample a minibatch of states in  $B_a$  where  $\|\bar{w}_r - w_i\|_2 > 1$ . We use a more generalized OOD metric called Mahalanobis distance later in §6.2, and we achieved similar results using it in this environment. Nevertheless, we present the results in this environment using L2 distance to show that LCPO can operate with a variety of OOD metrics.

Episodic reward across the online experiment is presented in Figure 6, and summarized statistics are presented in Table 1. All LCPO variants maintain a lead across input traces (with the exception of LCPO-P, which is surpassed by SAC on input 1). We observe that LCPO-S and LCPO-D are very close, and thus given the computational complexity, LCPO-S is more favored. LCPO-P is constantly outperformed by LCPO-S, which is likely because LCPO-P does not guarantee any anchoring and crudely balances improving the policy and not changing past output. We observe that in input 1 and 2, LCPO-S surpasses the best offline trained model, despite our carefully tuned offline trained models. This can be attributed to two reasons: 1) Only past wind is observed, not the current wind in the next transition. Since there is a small degree of

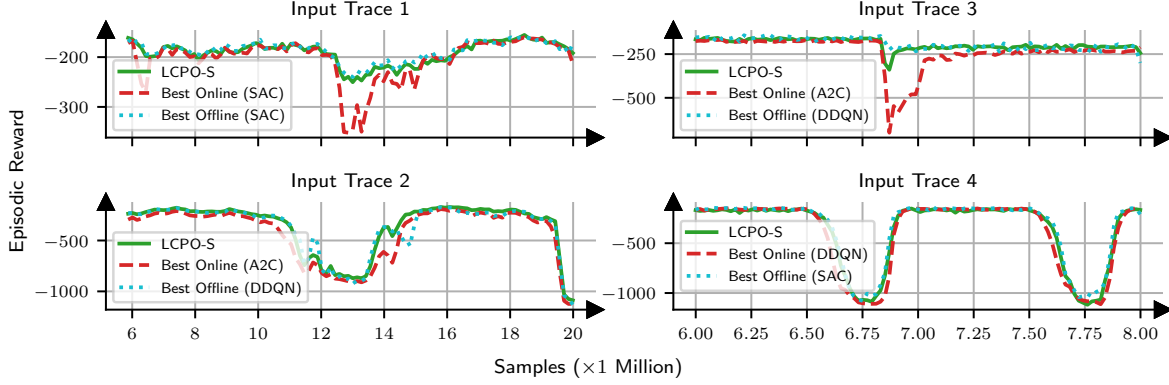


Figure 6. Episodic rewards as training progresses. We consider an initial learning period of 30000 episodes (6 million samples).

Table 1. Average episodic reward for different algorithms and conditions in the Pendulum-v1 environment with external wind processes.

	Online Training							Offline Training			
	LCPO-S	LCPO-D	LCPO-P	A2C	TRPO	DDQN	SAC	A2C	TRPO	DDQN	SAC
Input Trace 1	<b>-191</b>	-191	-211	-206	-227	-216	-204	-208	-203	-189	<b>-187</b>
Input Trace 2	<b>-356</b>	-356	-386	-420	-531	-561	-567	-404	-411	<b>-366</b>	-378
Input Trace 3	<b>-194</b>	-195	-224	-238	-343	-504	-430	-212	-194	<b>-189</b>	-210
Input Trace 4	<b>-375</b>	-380	-392	-413	-660	-405	-420	-387	-407	-370	<b>-349</b>

change from past wind to the current wind, this problem is minutely partially observable. A parallel agent has to consider an implicit universal model for these input transitions, while an online agent can fine-tune on the go to current transitions. 2) We use NNs with 2 hidden layers and 64 neurons in each. Even though this is in line with prior evaluations in this environment, larger neural networks might garner better results. Overall, LCPO-S manages to exploit the OOD metric and outperform even off-policy approaches in this problem.

## 6.2. Straggler mitigation with real inputs

We consider a non-stationary systems environment from prior work (Hamadanian et al., 2022), tasked with reducing tail latency response times in an online service (Figure 7). In this environment, an RL agent must select a timeout for incoming requests. If requests are not completed by their timeout, they will be replicated on a different server. If the replicated request finishes faster than the original one, the request’s latency is reduced. Replications incur extra load that can increase response time for later requests. Therefore, there is a balance between mitigating slow stragglers and inflating future response times. The optimal timeout depends on two factors: 1) how congested the servers are with other requests, and 2) the input (workload), i.e. request arrival rate and processing time. The input changes with time, as observed in real inputs visualized in Figure 8, leading to a non-stationary environment. Note that even as a human it is difficult to infer separate task labels, particularly for input 1.

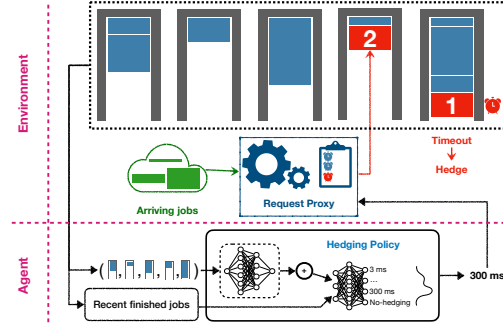


Figure 7. Illustration of a request proxy with hedging.

Every 500ms, the hedging policy gets to pick among a set of eight timeout values, ranging from 3ms to 1000ms, or alternatively to do no hedging. The reward is the 95<sup>th</sup> percentile latency of requests completed in that duration. The observation space is 32-dimensional, consisting of server queue lengths and workload statistics at several time-scales. For workloads, we use input traces provided by authors in (Hamadanian et al., 2022), that are from a production web framework cluster at AnonCo, collected from a single day in February 2018.

For the OOD metric  $W(B_a, B_r)$ , we fit a Gaussian multivariate model to the recent batch  $B_r$ , and report a minibatch of states in  $B_a$  with a Mahalanobis distance further than  $M$  from this distribution. LCPO-S Agg, LCPO-S Med and LCPO-S Cons use  $M = -5, -6$  and  $-7$ . A lower value

Table 2. Tail latency for different algorithms and input traces in the straggler mitigation environment.

	Online Training							Offline Training			
	LCPO-S Agg	LCPO-S Med	LCPO-S Cons	A2C	TRPO	DDQN	SAC	A2C	TRPO	DDQN	SAC
Input Trace 1	1067	<b>1054</b>	1056	1664	2924	1707	1955	1027	<b>984</b>	1319	2905
Input Trace 2	587	<b>561</b>	574	562	879	631	649	<b>509</b>	518	627	589

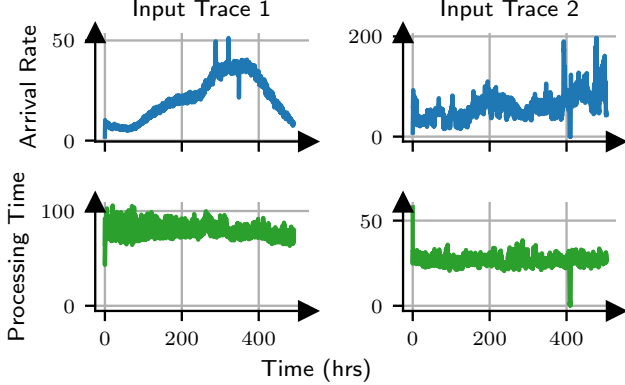


Figure 8. Request arrival rate and processing time per input.

for  $M$  yields more conservative OOD samples, hence the naming. The difference between these three is significant: The model in LCPO-S Agg allows for  $26.7x$  more samples to be considered OOD compared to LCPO-S Cons. While there are better ways to model workload distributions in such problems, we use Mahalanobis distance as it is a well-accepted and general approach for outlier detection in prior work (Lee et al., 2018; Podolskiy et al., 2021).

Tail latency across experiment time is presented in Figure 9, and Table 2 provides summarized statistics. We observe that all variations of LCPO-S achieve similar results. In input 1, LCPO-S vastly outperforms baselines, while in input 2, it outperforms 3 baselines, and slightly outperforms A2C. These results suggest that a locally constrained optimization strategy based on past OOD samples can mitigate performance loss due to catastrophic forgetting in this online system. The extreme stochasticity of this environment challenges state-of-the-art off-policy algorithms, leading to substantial gaps, even with respect to on-policy baselines. Note that unlike the framework in (Hamadani et al., 2022), our approach does not require manually designed workload clustering or oracle labels; we only require an OOD sampler.

## 7. Conclusion

We proposed and evaluated LCPO, a simple approach for learning policies in non-stationary environments. Using LCPO requires two conditions: 1) the non-stationarity must be induced by an exogenous observed input process; and

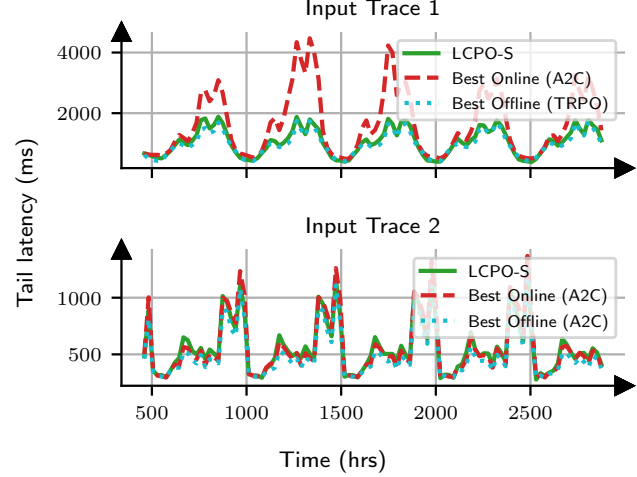


Figure 9. Tail latency as training progresses (lower is better). We consider an initial learning period of 27000 epochs.

2) a similarity metric is required that can inform us if two inputs come from noticeably different distributions (OOD detection). This is a weaker and simpler condition than requiring task labels (context detection) as it does not require explicit classification. We observed that LCPO is capable of outperforming baselines on two environments with real and synthetic input traces. These inputs spanned multiple behaviors, from sudden dramatic shifts to smoothly and slowly changing distributions.

LCPO focuses on mitigating catastrophic forgetting in online non-stationary RL. An orthogonal challenge in this setting is efficient exploration, i.e. explore when the input distribution has changed but only explore once per new input distribution. Our experiments used automatic entropy tuning for exploration as done with SAC (Haarnoja et al., 2018b). While empirically effective, this approach was not designed for non-stationary problems, and LCPO may benefit from a better exploration methodology.

LCPO comes in three flavors; doubly-constrained trust region optimization, singly-constrained trust region optimization, and proximal policy optimization with a proxy loss for locally constraining the policy. While LCPO-S proved to be the best overall, their performance demonstrates that locally constraining the policy can be carried out in a variety of ways, and is not tied to one specific RL algorithm.



## References

- Alegre, L. N., Bazzan, A. L., and da Silva, B. C. Minimum-delay adaptation in non-stationary reinforcement learning via online high-confidence change-point detection. In *Proceedings of the 20th International Conference on Autonomous Agents and MultiAgent Systems*, pp. 97–105, 2021.
- Atkinson, C., McCane, B., Szymanski, L., and Robins, A. Pseudo-rehearsal: Achieving deep reinforcement learning without catastrophic forgetting. *Neurocomputing*, 428:291–307, Mar 2021. ISSN 0925-2312. doi: 10.1016/j.neucom.2020.11.050. URL <http://dx.doi.org/10.1016/j.neucom.2020.11.050>.
- Brockman, G., Cheung, V., Pettersson, L., Schneider, J., Schulman, J., Tang, J., and Zaremba, W. Openai gym. *arXiv preprint arXiv:1606.01540*, 2016.
- da Silva, B. C., Basso, E. W., Bazzan, A. L. C., and Engel, P. M. Dealing with non-stationary environments using context detection. In *Proceedings of the 23rd International Conference on Machine Learning, ICML '06*, pp. 217–224, New York, NY, USA, 2006. Association for Computing Machinery. ISBN 1595933832. doi: 10.1145/1143844.1143872. URL <https://doi.org/10.1145/1143844.1143872>.
- Doya, K., Samejima, K., Katagiri, K.-i., and Kawato, M. Multiple model-based reinforcement learning. *Neural computation*, 14(6):1347–1369, 2002.
- Duan, Y., Chen, X., Houthoofd, R., Schulman, J., and Abbeel, P. Benchmarking deep reinforcement learning for continuous control. In *International conference on machine learning*, pp. 1329–1338. PMLR, 2016.
- Farajtabar, M., Azizan, N., Mott, A., and Li, A. Orthogonal gradient descent for continual learning, 2019. URL <https://arxiv.org/abs/1910.07104>.
- Gu, S., Lillicrap, T., Ghahramani, Z., Turner, R. E., and Levine, S. Q-prop: Sample-efficient policy gradient with an off-policy critic. *arXiv preprint arXiv:1611.02247*, 2016.
- Gu, Z., She, C., Hardjawana, W., Lumb, S., McKechnie, D., Essery, T., and Vucetic, B. Knowledge-assisted deep reinforcement learning in 5g scheduler design: From theoretical framework to implementation. *IEEE Journal on Selected Areas in Communications*, 39(7):2014–2028, 2021.
- Haarnoja, T., Pong, V., Zhou, A., Dalal, M., Abbeel, P., and Levine, S. Composable deep reinforcement learning for robotic manipulation. In *2018 IEEE International Conference on Robotics and Automation (ICRA)*, pp. 6244–6251, 2018a. doi: 10.1109/ICRA.2018.8460756.
- Haarnoja, T., Zhou, A., Abbeel, P., and Levine, S. Soft actor-critic: Off-policy maximum entropy deep reinforcement learning with a stochastic actor. In *International conference on machine learning*, pp. 1861–1870. PMLR, 2018b.
- Haarnoja, T., Zhou, A., Hartikainen, K., Tucker, G., Ha, S., Tan, J., Kumar, V., Zhu, H., Gupta, A., Abbeel, P., and Levine, S. Soft actor-critic algorithms and applications, 2018c. URL <https://arxiv.org/abs/1812.05905>.
- Hamadani, P., Schwarzkopf, M., Sen, S., and Alizadeh, M. Demystifying reinforcement learning in time-varying systems, 2022. URL <https://arxiv.org/abs/2201.05560>.
- Hasselt, H. v., Guez, A., and Silver, D. Deep reinforcement learning with double q-learning. In *Proceedings of the Thirtieth AAAI Conference on Artificial Intelligence, AAAI'16*, pp. 2094–2100. AAAI Press, 2016.
- Haydari, A. and Yilmaz, Y. Deep reinforcement learning for intelligent transportation systems: A survey. *IEEE Transactions on Intelligent Transportation Systems*, 23(1):11–32, 2022. doi: 10.1109/TITS.2020.3008612.
- Heess, N., TB, D., Sriram, S., Lemmon, J., Merel, J., Wayne, G., Tassa, Y., Erez, T., Wang, Z., Eslami, S. M. A., Riedmiller, M., and Silver, D. Emergence of locomotion behaviours in rich environments, 2017. URL <https://arxiv.org/abs/1707.02286>.
- Isele, D. and Cosgun, A. Selective experience replay for lifelong learning, 2018.
- Kaplanis, C., Shanahan, M., and Clopath, C. Continual reinforcement learning with complex synapses, 2018.
- Khetarpal, K., Riemer, M., Rish, I., and Precup, D. Towards continual reinforcement learning: A review and perspectives. *arXiv preprint arXiv:2012.13490*, 2020.
- Kingma, D. P. and Ba, J. Adam: A method for stochastic optimization, 2017.
- Kirkpatrick, J., Pascanu, R., Rabinowitz, N., Veness, J., Desjardins, G., Rusu, A. A., Milan, K., Quan, J., Ramalho, T., Grabska-Barwinska, A., et al. Overcoming catastrophic forgetting in neural networks. *Proceedings of the national academy of sciences*, 114(13):3521–3526, 2017.
- Lee, K., Lee, K., Lee, H., and Shin, J. A simple unified framework for detecting out-of-distribution samples and adversarial attacks, 2018. URL <https://arxiv.org/abs/1807.03888>.
- Mao, H., Netravali, R., and Alizadeh, M. Neural adaptive video streaming with pensieve. In *Proceedings of the*

- Conference of the ACM Special Interest Group on Data Communication, pp. 197–210, 2017.
- Mao, H., Schwarzkopf, M., Venkatakrisnan, S. B., Meng, Z., and Alizadeh, M. Learning scheduling algorithms for data processing clusters, 2018a. URL <https://arxiv.org/abs/1810.01963>.
- Mao, H., Venkatakrisnan, S. B., Schwarzkopf, M., and Alizadeh, M. Variance reduction for reinforcement learning in input-driven environments, 2018b. URL <https://arxiv.org/abs/1807.02264>.
- Mao, H., Schwarzkopf, M., Venkatakrisnan, S. B., Meng, Z., and Alizadeh, M. Learning scheduling algorithms for data processing clusters. In *Proceedings of the ACM Special Interest Group on Data Communication, SIGCOMM '19*, pp. 270–288, New York, NY, USA, 2019. Association for Computing Machinery. ISBN 9781450359566. doi: 10.1145/3341302.3342080. URL <https://doi.org/10.1145/3341302.3342080>.
- Marcus, R., Negi, P., Mao, H., Zhang, C., Alizadeh, M., Kraska, T., Papaemmanouil, O., and Tatbul, N. Neo: A learned query optimizer. *arXiv preprint arXiv:1904.03711*, 2019.
- McCloskey, M. and Cohen, N. J. Catastrophic interference in connectionist networks: The sequential learning problem. *Psychology of Learning and Motivation*, 24:109–165, 1989. ISSN 0079-7421. doi: [https://doi.org/10.1016/S0079-7421\(08\)60536-8](https://doi.org/10.1016/S0079-7421(08)60536-8). URL <https://www.sciencedirect.com/science/article/pii/S0079742108605368>.
- Mnih, V., Kavukcuoglu, K., Silver, D., Graves, A., Antonoglou, I., Wierstra, D., and Riedmiller, M. Playing atari with deep reinforcement learning. *arXiv preprint arXiv:1312.5602*, 2013.
- Mnih, V., Badia, A. P., Mirza, M., Graves, A., Lillicrap, T., Harley, T., Silver, D., and Kavukcuoglu, K. Asynchronous methods for deep reinforcement learning. In *International conference on machine learning*, pp. 1928–1937. PMLR, 2016.
- Nagabandi, A., Finn, C., and Levine, S. Deep online learning via meta-learning: Continual adaptation for model-based rl, 2019.
- Padakandla, S., J., P. K., and Bhatnagar, S. Reinforcement learning algorithm for non-stationary environments. *Applied Intelligence*, 50(11):3590–3606, jun 2020. doi: 10.1007/s10489-020-01758-5. URL <https://doi.org/10.1007/s10489-020-01758-5>.
- Parisi, G. I., Kemker, R., Part, J. L., Kanan, C., and Wermter, S. Continual lifelong learning with neural networks: A review. *Neural Networks*, 113:54–71, 2019. ISSN 0893-6080. doi: <https://doi.org/10.1016/j.neunet.2019.01.012>. URL <https://www.sciencedirect.com/science/article/pii/S0893608019300231>.
- Paszke, A., Gross, S., Massa, F., Lerer, A., Bradbury, J., Chanan, G., Killeen, T., Lin, Z., Gimelshein, N., Antiga, L., Desmaison, A., Kopf, A., Yang, E., DeVito, Z., Raison, M., Tejani, A., Chilamkurthy, S., Steiner, B., Fang, L., Bai, J., and Chintala, S. Pytorch: An imperative style, high-performance deep learning library. In Wallach, H., Larochelle, H., Beygelzimer, A., d'Alché-Buc, F., Fox, E., and Garnett, R. (eds.), *Advances in Neural Information Processing Systems 32*, pp. 8024–8035. Curran Associates, Inc., 2019. URL <http://papers.neurips.cc/paper/9015-pytorch-an-imperative-style-high-performance-deep-learning-library.pdf>.
- Pathak, D., Agrawal, P., Efros, A. A., and Darrell, T. Curiosity-driven exploration by self-supervised prediction, 2017. URL <https://arxiv.org/abs/1705.05363>.
- Pinto, L., Davidson, J., Sukthankar, R., and Gupta, A. Robust adversarial reinforcement learning, 2017. URL <https://arxiv.org/abs/1703.02702>.
- Podolskiy, A., Lipin, D., Bout, A., Artemova, E., and Piontkovskaya, I. Revisiting mahalanobis distance for transformer-based out-of-domain detection, 2021. URL <https://arxiv.org/abs/2101.03778>.
- Raffin, A. RL baselines3 zoo. <https://github.com/DLR-RM/rl-baselines3-zoo>, 2020.
- Raffin, A., Hill, A., Gleave, A., Kanervisto, A., Ernestus, M., and Dormann, N. Stable-baselines3: Reliable reinforcement learning implementations. *Journal of Machine Learning Research*, 22(268):1–8, 2021. URL <http://jmlr.org/papers/v22/20-1364.html>.
- Ren, H., Sootla, A., Jafferjee, T., Shen, J., Wang, J., and Bou Ammar, H. Reinforcement learning in presence of discrete markovian context evolution, 02 2022.
- Rolnick, D., Ahuja, A., Schwarz, J., Lillicrap, T. P., and Wayne, G. Experience replay for continual learning, 2019.
- Rusu, A. A., Rabinowitz, N. C., Desjardins, G., Soyer, H., Kirkpatrick, J., Kavukcuoglu, K., Pascanu, R., and Hadsell, R. Progressive neural networks. *arXiv preprint arXiv:1606.04671*, 2016.
- Schulman, J., Levine, S., Moritz, P., Jordan, M. I., and Abbeel, P. Trust region policy optimization, 2015. URL <https://arxiv.org/abs/1502.05477>.

- Schulman, J., Wolski, F., Dhariwal, P., Radford, A., and Klimov, O. Proximal policy optimization algorithms, 2017. URL <https://arxiv.org/abs/1707.06347>.
- Schulman, J., Moritz, P., Levine, S., Jordan, M., and Abbeel, P. High-dimensional continuous control using generalized advantage estimation, 2018.
- Schwarz, J., Luketina, J., Czarnecki, W. M., Grabska-Barwinska, A., Teh, Y. W., Pascanu, R., and Hadsell, R. Progress & compress: A scalable framework for continual learning, 2018.
- Sinitisin, A., Plokhotnyuk, V., Pyrkun, D., Popov, S., and Babenko, A. Editable neural networks, 2020. URL <https://arxiv.org/abs/2004.00345>.
- Sutton, R. S. and Barto, A. G. *Reinforcement Learning: An Introduction*. A Bradford Book, Cambridge, MA, USA, 2018. ISBN 0262039249.
- Tang, Y. and Agrawal, S. Discretizing continuous action space for on-policy optimization, 2019. URL <https://arxiv.org/abs/1901.10500>.
- Uhlenbeck, G. E. and Ornstein, L. S. On the theory of the brownian motion. *Phys. Rev.*, 36:823–841, Sep 1930. doi: 10.1103/PhysRev.36.823. URL <https://link.aps.org/doi/10.1103/PhysRev.36.823>.
- Zhang, H., Zhou, A., Hu, Y., Li, C., Wang, G., Zhang, X., Ma, H., Wu, L., Chen, A., and Wu, C. Loki: Improving long tail performance of learning-based real-time video adaptation by fusing rule-based models. In *Proceedings of the 27th Annual International Conference on Mobile Computing and Networking*, MobiCom '21, pp. 775–788, New York, NY, USA, 2021. Association for Computing Machinery. ISBN 9781450383424. doi: 10.1145/3447993.3483259. URL <https://doi.org/10.1145/3447993.3483259>.
- Zhu, H., Yu, J., Gupta, A., Shah, D., Hartikainen, K., Singh, A., Kumar, V., and Levine, S. The ingredients of real-world robotic reinforcement learning, 2020. URL <https://arxiv.org/abs/2004.12570>.

## A. LCPO

### A.1. LCPO-D: Solving two constraints

We intend to solve the following optimization problem:

$$\begin{aligned} \min_x \quad & x^T v \\ \text{s.t.} \quad & x^T A x \leq c_a \\ \text{s.t.} \quad & x^T B x \leq c_b \end{aligned} \quad (5)$$

We can form the lagrangian dual of the problem:

$$\begin{aligned} \max_{\lambda_a, \lambda_b} \min_x \quad & x^T v + \lambda_a (x^T A x - c_a) + \lambda_b (x^T B x - c_b) \\ \text{s.t.} \quad & \lambda_a, \lambda_b \geq 0 \end{aligned} \quad (6)$$

We have one feasible solution ( $x=0$ ) and our optimization problem is convex. Thus KKT conditions apply and we have for the solution to the above ( $x^*, \lambda_a^*, \lambda_b^*$ ):

$$\begin{aligned} v + \lambda_a^* 2A x^* + \lambda_b^* 2B x^* &= 0 \\ \Rightarrow x^* &= 2\lambda_a^* A^{-1} v + 2\lambda_b^* B^{-1} v \end{aligned} \quad (7)$$

Note that  $A$  and  $B$  are Hessian matrices and symmetric ( $A^T = A$ ). In practice, we can't calculate  $A$  and  $B$  due to their size, let alone their inverses. Instead, we can calculate two general derivations of them. First, we can calculate  $Av$  without materializing the entire matrix  $A$  in memory with this trick:

$$\begin{aligned} Av &= \nabla_x^2 D_{KL}(x, 0, \cdot)|_0 \cdot v \\ &= \nabla_x (v^T \cdot \nabla_x D_{KL}(x, 0, \cdot)|_0)|_0 \end{aligned} \quad (8)$$

Second, using the above and the conjugate gradient theorem, we can calculate  $x_a := A^{-1}v$  and  $x_b := B^{-1}v$ . Now we have:

$$x^* = 2\lambda_a^* x_a + 2\lambda_b^* x_b \quad (9)$$

We can plug this back to our conditions:

$$\begin{aligned} x^{*T} A x^* &= (2\lambda_a^* x_a + 2\lambda_b^* x_b)^T A (2\lambda_a^* x_a + 2\lambda_b^* x_b) \\ &= 4\lambda_a^{*2} v^T x_a + 4\lambda_a^* \lambda_b^* v^T x_b + 4\lambda_b^{*2} x_b^T B x_b \\ &= t_1 \lambda_a^{*2} + r_1 \lambda_a^* \lambda_b^* + s_1 \lambda_b^{*2} = c_b \end{aligned} \quad (10)$$

And similarly:

$$\begin{aligned} x^{*T} B x^* &= (2\lambda_a^* x_a + 2\lambda_b^* x_b)^T B (2\lambda_a^* x_a + 2\lambda_b^* x_b) \\ &= 4\lambda_a^{*2} x_a^T B x_a + 4\lambda_a^* \lambda_b^* v^T x_a + 4\lambda_b^{*2} v^T x_b \\ &= t_2 \lambda_a^{*2} + r_2 \lambda_a^* \lambda_b^* + s_2 \lambda_b^{*2} = c_b \end{aligned} \quad (11)$$

Now we reparametrize  $u = \frac{\lambda_a^*}{\lambda_b^*}$  (we implicitly assume that  $\lambda_b \neq 0$ , as that case can be easily checked), and we have:

$$\begin{aligned} t_1 u^2 + r_1 u + s_1 &= \frac{c_a}{\lambda_b^{*2}} \\ t_2 u^2 + r_2 u + s_2 &= \frac{c_b}{\lambda_b^{*2}} \\ \Rightarrow (t_1 - \frac{c_a t_2}{c_b}) u^2 + (r_1 - \frac{c_a r_2}{c_b}) u + (s_1 - \frac{c_a s_2}{c_b}) &= 0 \end{aligned} \quad (12)$$

If the equation above does not have a real solution, we can not satisfy both constraints. Since we know this problem has at least one solution ( $x=0$ ), this means that one of these constraints will always lead to the other being satisfied. In that case, we revert to using one constraint and applying the other via the line search stage.

Alternatively, this equation might have only one or two negative solutions, which as both  $\lambda_a^*$  and  $\lambda_b^*$  are non-negative, is not acceptable. This leads us to the same conclusion as before.

Next, this equation might have two non-negative solutions. Both solutions perfectly fit the constraints, and minimize the optimization objective. Either could be chosen. Lastly, when the equation has one non-negative solution, we use it to compute  $x^*$ .

## B. Pendulum Locomotion

### B.1. Action Space

Pendulum by default has a continuous action space, ranging from  $-2$  to  $2$ . We observed instability while learning policies with continuous policy classes even without external wind, and were concerned about how this can affect the validity of our experiments with wind, which are considerably more challenging. As the action space is tangent to our problem, we discretized the action space to 15 atoms, spaced equally from  $-2$  to  $2$ . This stabilized training greatly, and is not surprising, as past work (Tang & Agrawal, 2019) supports this observation. The reward metric, continuous state space and truncation and termination conditions remain unchanged.

We provide the achieved reward for all baselines in §6 in Table 3, over 5 seeds. A2C, DDQN and SAC were trained for 8000 epochs, and TRPO was trained for 500 epochs. Evaluations are on 1000 episodes. As these results show, the agents exhibit stable training with a discretized action space.

### B.2. Experiment Setup

We use OpenAI Gym (v0.26.2). Our implementations of A2C, TRPO, DDQN and SAC use the Pytorch (Paszke et al., 2019) library. Table 4 is a comprehensive list of all



Table 3. Average episodic reward for different algorithms in the Pendulum-v1 environment with discretized and continuous action space.

Episodic Reward	A2C	TRPO	DDQN	SAC
Discrete	-167	-165	-149	-146
SB3 (Raffin et al., 2021) + RL-Zoo (Raffin, 2020)	-203	-224	—	-176

hyperparameters used in training and the environment.

## C. Straggler mitigation

### C.1. Experiment Setup

We use the straggler mitigation environment from prior work (Hamadani et al., 2022), with a similar configuration except with 9 actions (timeouts of  $600^{ms}$  and  $1000^{ms}$  added). Similar to §B.2, our implementations of A2C, TRPO, DDQN and SAC use the Pytorch (Paszke et al., 2019) library. Table 5 is a comprehensive list of all hyperparameters used in training and the environment.

Table 4. Training setup and hyperparameters for Pendulum-v1 with external wind.

Group	Hyperparameter	Value
Neural network	Hidden layers	(64, 64)
	Hidden layer activation function	Relu
	Output layer activation function	Actors: Softmax, Critics and DDQN: Identity mapping
	Optimizer	Adam ( $\beta_1 = 0.9, \beta_2 = 0.999$ ) (Kingma & Ba, 2017)
	Learning rate	Actor: 0.0004, Critic and DDQN: 0.001
	Weight decay	$10^{-4}$
RL training (general)	Random seeds	5
	$\lambda$ (for GAE in A2C and TRPO)	0.9
	$\gamma$	0.99
A2C	Rollout per epoch	200
TRPO	Rollout per epoch	3200
	Damping coefficient	0.1
	Stepsize	0.01
DDQN	Rollout per epoch	200
	Batch Size	512
	Initial fully random period	1000 epochs
	$\epsilon$ -greedy schedule	1 to 0 in 5000 epochs
	Polyak $\alpha$	0.01
	Buffer size $N$	All samples ( $N = 20M$ or $N = 8M$ )
SAC	Rollout per epoch	200
	Batch Size	512
	Initial fully random period	1000 epochs
	Base Entropy	0.1
	Entropy Target	$0.1 \ln(15)$
	Log-Entropy Learning Rate	$1e-3$
	Polyak $\alpha$	0.01
LCPO (-P, -S, -D)	Buffer size $N$	All samples ( $N = 20M$ or $N = 8M$ )
	Rollout per epoch	200
	Base Entropy	0.03
	Entropy Target	$0.1 \ln(15)$
LCPO-S and LCPO-D	Log-Entropy Learning Rate	$1e-3$
	Damping coefficient	0.1
	$c_{anchor}$	0.0001
LCPO-P	$c_{recent}$	0.1
	PPO Clipping $\epsilon$	0.2
	PPO Iterations (Max)	30
	PPO Max KL	0.01
	$\kappa$	10

Table 5. Training setup and hyperparameters for straggler mitigation experiments.

Group	Hyperparameter	Value
Neural network	Hidden layers	$\phi$ network: (32, 16) $\rho$ network: (32, 32)
	Hidden layer activation function	Relu
	Output layer activation function	Actors: Softmax, Critics and DDQN: Identity mapping
	Optimizer	Adam ( $\beta_1 = 0.9, \beta_2 = 0.999$ ) (Kingma & Ba, 2017)
	Learning rate	0.001
	Weight decay	$10^{-4}$
RL training (general)	Random seeds	5
	$\lambda$ (for GAE in A2C and TRPO)	0.95
	$\gamma$	0.9
A2C	Rollout per epoch	4608
TRPO	Rollout per epoch	10240
	Damping coefficient	0.1
	Stepsize	0.01
DDQN	Rollout per epoch	128
	Batch Size	512
	Initial fully random period	1000 epochs
	$\epsilon$ -greedy schedule	1 to 0 in 5000 epochs
	Polyak $\alpha$	0.01
	Buffer size $N$	All samples ( $N = 21M$ )
SAC	Rollout per epoch	128
	Batch Size	512
	Initial fully random period	1000 epochs
	Base Entropy	0.01
	Entropy Target	$0.1 \ln(9)$
	Log-Entropy Learning Rate	1e-3
	Polyak $\alpha$	0.005
	Buffer size $N$	All samples ( $N = 21M$ )
LCPO-S	Rollout per epoch	128
	Base Entropy	0.01
	Entropy Target	$0.1 \ln(9)$
	Log-Entropy Learning Rate	1e-3
	Damping coefficient	0.1
	$c_{anchor}$	0.0001
	$c_{recent}$	0.1